# Beam-Pointing Verification Using X-Ray Pinhole Cameras on the 60-Beam OMEGA Laser

C. Stoeckl, D. Cao, L. Ceurvorst, A. Kalb, J. Kwiatkowski, A. Shvydky, and W. Theobald

Laboratory for Laser Energetics, University of Rochester

On the OMEGA Laser System, the beam-pointing accuracy is verified by irradiating a 4-mm-diam Au-coated spherical target with ~23 kJ of laser energy.[1] Up to ten x-ray pinhole cameras record the emission from all 60 beam spots [see Fig. 1(a)]. A new set of algorithms has been developed to improve the accuracy of the pointing evaluation. An updated edge-finding procedure allows one to infer the center of the sphere with subpixel accuracy. A new approach was introduced to back-propagate the pixel locations on the 2-D image to the 3-D surface of the sphere. A fast Fourier transform-based noise reduction method significantly improves the signal-to-noise ratio of the data. Based on the beam-pointing analysis, hard-sphere calculations of the laser-drive illumination uniformity on the target surface and the decomposition of the illumination distribution into lower order modes (1 to 10) are evaluated.

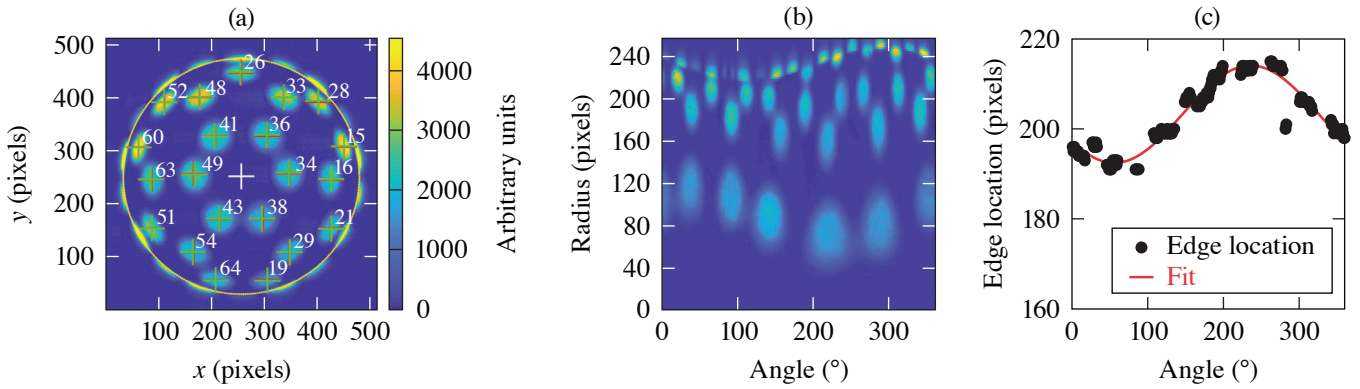


Figure 1
(a) X-ray image from one of the ten x-ray pinhole cameras acquired during a pointing shot. The position of up to 21 beams can be evaluated (red crosses) and compared to the desired locations (green crosses). The white cross shows the evaluated center of the sphere and the yellow circle is the outside radius. (b) Angular lineouts from a first guess of the center of the image of the sphere. (c) Evaluated location of the edge of the sphere compared to a cosine fit.

To infer the location of the center of the sphere, radial lineouts starting from a first estimate of the center $(x_e, y_e)$ of the image are taken in 1° angular increments. Figure 1(b) shows a composite of these lineouts in the form of a 2-D image. The edge feature from the self-shadowing of the beams behind the horizon can be clearly seen at the top of the image. The location of the edge is determined as the position of the maximum of the gradient of each lineout and plotted in Fig. 2(c). Lines with low signal or high noise are discarded. A cosine function of the form $r = r_0 + a * \cos(t + b)$ is fitted to the data, with $t$ as the angle, $b$ as the phase offset, and $a$ as the amplitude of the radial variation. From simple geometry, two offsets $(dx, dy)$ can be computed that correct the estimated center to provide a better fit of the center $x_f = x_e + dx$; $y_f = y_e + dy$. Depending on the magnitude of the radial variation, this process can be repeated to get the best fit of the center.

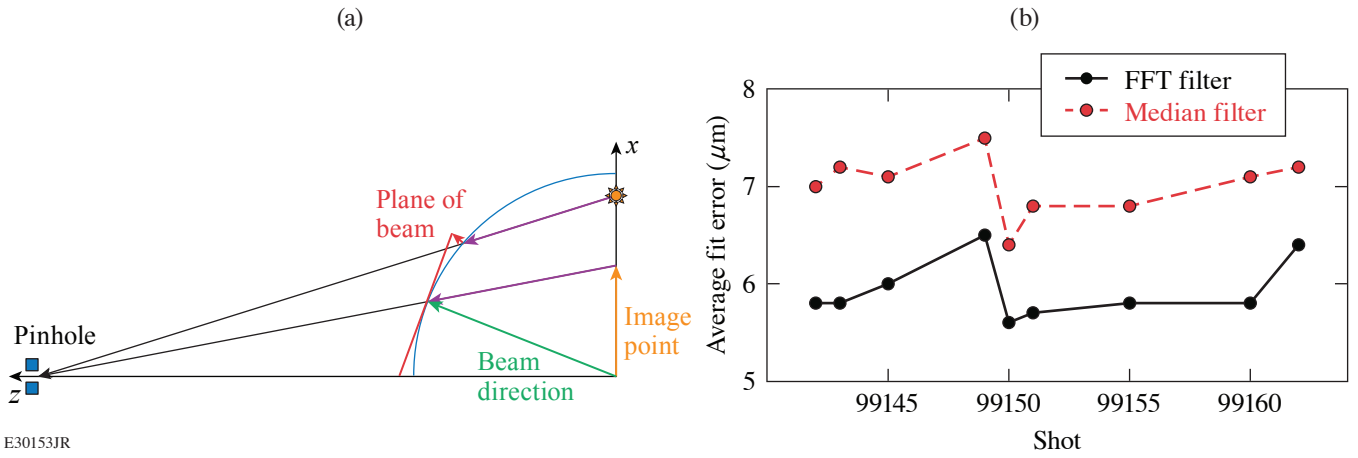


Figure 2
(a) Sketch of the geometry used to project the emission recorded from the individual beams into the planes perpendicular to the beam propagation direction. (b) Average pointing error evaluated from a median filtered image compared to a fast Fourier transform (FFT)-filtered image.

The x-ray pinhole camera image is a 2-D projection of the emission from a 3-D sphere. To infer the intensity distribution on the sphere, the image from the sensor is mapped to the object plane through the pinhole, and then each pixel location is projected onto the sphere [see purple arrow in Fig. 2(a)]. Since the intensity distribution of the laser focus is defined in a plane perpendicular to the laser propagation direction, the pixel locations on the sphere for a single beam are further projected onto the plane perpendicular to the laser direction tangent to the surface of the sphere [red arrow in Fig. 2(a)]. This procedure corrects all geometric effects of the imaging and compensates the ellipticity of the beams close to the edge of the image very well.

Simple median filters are typically used to clean up the raw charge-injection–device (CID) images under the assumption that the noise seen is purely statistical and uncorrelated. Upon more-detailed inspection of the images, it became obvious that there are medium- and large-scale correlations in the noise mostly caused by imperfections in the readout system. To clean up these correlated features a 2-D FFT is generated from the image and the regions in the FFT corresponding to high spatial frequencies or clearly identifiable background features are set to zero. A cleaned-up image is then reconstructed using the inverse FFT. The evaluation of the pointing with the FFT filtered images show a significant improvement in fit error [see Fig. 2(b)].

The limiting factors on the accuracy of the pointing evaluation, which are currently of the order of 5 $\mu$m, are most likely the quality of the pointing targets, noise (especially correlated features) in the CID readout, and imperfections in the intensity distribution of the laser beam focus. A more-uniform coating for of targets would reduce the artifacts in the image, like the "holes" [as seen in Fig. 1(a)], and lead to better fits. It is also likely that the FFT filter can be further improved by using an evolutionary algorithm or a machine learning approach.

This material is based upon work supported by the Department of Energy National Nuclear Security Administration under Award Number DE-NA0003856, the University of Rochester, and the New York State Energy Research and Development Authority.

1. R. A. Forties and F. J. Marshall, Rev. Sci. Instrum. **76**, 073505 (2005).